engineering proceedings

MDPI

Proceeding Paper

Learning the Buckled Geometry of 3D Printed Stiffeners of Pre-Stretched Soft Membranes †

Simone Battisti, Daniel Calegaro, Paolo Marcandelli, Alice Todeschini * and Stefano Mariani

Department of Civil and Environmental Engineering, Politecnico di Milano, Piazza L. da Vinci 32, 20133 Milano, Italy; simone.battisti@mail.polimi.it (S.B.); daniel.calegaro@polimi.it (D.C.); paolo.marcandelli@polimi.it (P.M.); stefano.mariani@polimi.it (S.M.)

* Correspondence: alice.todeschini@mail.polimi.it

† Presented at the 2nd International Electronic Conference on Machines and Applications, 18–20 June, 2024; Available online: https://sciforum.net/event/IECMA2024.

Abstract: A deep learning strategy was exploited to learn and predict the deformation of stiffeners, 3D printed onto a pre-stretched soft membrane. The working process reads as follows: the membrane is stretched until a pre-defined level; a specific geometry of stiffeners is printed onto it; the membrane is finally released, and due to the presence of the printed stiffeners, the system undergoes an out-of-plane deformation due to buckling. Fused deposition modeling was specifically calibrated to print PLA (Polylactic acid or polylactide) on a Lycra fabric. To assess how the printed pattern affects the buckled configuration, samples featuring different dimensions and in-plane geometries of the stiffeners were printed and numerically modeled via finite elements (FEs). The calibrated model was next exploited to construct a larger training dataset of stiffener geometries. A pre-trained You Only Look Once (YOLO)-based digital model was finally trained to foresee the link between the in-plane dimensions of the stiffeners before the release and the out-of-plane displacements in the buckled configuration. By handling around 100 different patterns, a precision of 93% in terms of recognition of the in-plane dimensions of the stiffeners and a mean absolute percentage error of 5% at most in terms of an estimate of the features of the buckled configuration were attained. The reported results testify the capability of the proposed approach and its potential efficiency to optimize the shape of the 3D printed geometries.

Keywords: 3D printing; smart textiles; deep learning; neural networks; YOLO

Citation: Battisti, S.; Calegaro, D.; Marcandelli, P.; Todeschini, A.; Mariani, S. Learning the Buckled Geometry of 3D Printed Stiffeners of Pre-Stretched Soft Membranes. *Eng. Proc.* **2024**, *72*, 3. https://doi.org/10.3390/engproc2024072003

Academic Editor: Antonio J. Marques Cardoso

Published: 23 September 2024

1. Introduction

The interplay between different materials under mechanical loading presents a unique set of challenges and opportunities. Several new possible applications can be unlocked by exploiting the time-varying interaction between stiffeners and a soft substrate, e.g., if the substrate itself is stretched before the stiffeners are introduced into the system [1–3]. Depending on the intended application, a variety of substrate and stiffener materials can be adopted [4], and different fabrication methods can be employed [5].

This research was specifically focused on the assessment of the deformation pattern of PLA stiffeners, 3D printed onto a pre-stretched Lycra membrane with a Voron 2.4 3D printer. Upon the release of the Lycra membrane, the printed geometries are shown to undergo different buckling-governed deformations; see, e.g., [6] for a thorough discussion on the theoretical bases of the current results. Such configurations are not only of theoretical interest but also have practical implications in the design and application of manufactured materials [7–9]. The printed geometry thus emerges as a key factor in the determination of the final shape, which plays on its own a critical role in meeting the requirements for the desired application.

To provide a comprehensive study on these effects, to understand the interaction between the pattern of the stiffeners and the buckled shape, and to then optimize the said

shape in order to attain (hopefully unprecedented) results, experimental tests carried out in the laboratory and the outcomes of FE analyses within an advanced computational frame are presented in this work. Numerical results were supplemented to the experimental ones, within a so-called multi-fidelity scheme [10], to enrich the dataset of solutions and drive the learning stage by way of a neural network (NN)-based scheme.

The deep learning (DL) approach harnessed the power of a pre-trained YOLO model to identify and quantify the in-plane dimensions of each printed geometry from pictures taken before the release of the pre-stretch. Subsequently, a regression network was exploited to predict the out-of-plane displacement of the stiffeners, effectively linking the observed geometric features with the resulting mechanical responses. Machine learning tools have already been adopted within the realm of 3D printing, to correlate the printing parameters to the characteristics of the final product, such as the mechanical properties and the surface roughness [11,12]. In this work, the focus was not on the 3D printed part but rather on the assessment of the interaction between the elastic properties of the substrate and stiffeners, aiming to create a digital twin able to predict the behavior of the entire system under a varying geometry of the 3D printed parts.

This multifaceted approach not only allows for enhancing the predictive capabilities of NNs in handling complex physical phenomena but also sets the stage for future developments in the optimization of 3D printed structures to attain targeted mechanical properties. The integration of machine learning strategies with traditional simulation, or physics-based techniques, see [13], can further pave the way for novel methodologies in the field of additive manufacturing, aiming to optimize material and structural responses for real-world applications.

The main novelty of the procedure proposed in this work stems from the integrated experimental and numerical approach to building a kind of cross-domain learning strategy (see e.g., [14]), aiming to encode the role of pre-stretch and the pattern/geometry of the 3D printed stiffeners in the buckled configuration. The remainder of this paper is thus arranged as follows: Section 2 reports the adopted solutions for 3D printing, numerical modeling of the joint response of soft substrate and stiffeners, and the learning of the resulting buckled configuration; Section 3 is devoted to the presentation and discussion of some results; finally, some concluding remarks and suggestions for future developments are gathered in Section 4.

2. Methods

Three-dimensional printing on textiles can be employed for the production of smart systems, even endowed with shape memory effects. When a material exhibits such effects, any stimulus inducing a specific trigger can lead to shape and function metamorphoses; if the trigger is removed, the material can return to its original shape. This feature is here obtained by extruding a thermoplastic polymer filament onto a flexible substrate, which is kept in tension during the printing process and then released.

When the textile is stretched, it also stores an internal (elastic) energy. If no parts are additionally printed on it, as soon as the tensile stress is released, the fabric returns to its original configuration. The interaction with the printed part acts instead as a constraint, resulting in the formation of a 3D buckled configuration that is induced by the balance of forces and moments. The so-formed structures usually show two or more metastable equilibrium states (multi-stable configurations) and are free to switch between them with the application of a small triggering stimulus. For these reasons, these textile systems can be labeled as *smart textiles*, meaning that they can purposely change their shape or function in response to the external actions, within a time-varying frame [7,15].

In the following, a discussion is reported on the methodology adopted in the laboratory to induce the sought buckled configuration of the smart textile, and the parameters mainly affecting the 3D printing process are discussed. Next, numerical simulations, carried out using the commercial finite element code Abaqus, are discussed to pinpoint the critical

issues in the analysis of such slender systems. Finally, the NN-based approach used to learn and predict the buckling behavior of the stiffened textile is described.

2.1. Additive Manufacturing

A VORON 2.4 3D printer was used to take advantage of its printable surface of dimensions 350 mm × 350 mm, using a printing bed made of aluminum. Results were obtained by extruding PLA on a pre-deformed sheet of Lycra. Figure 1 shows a picture of the 3D printer and a test setup adopted to uniaxially stretch the Lycra substrate before printing the stiffeners.

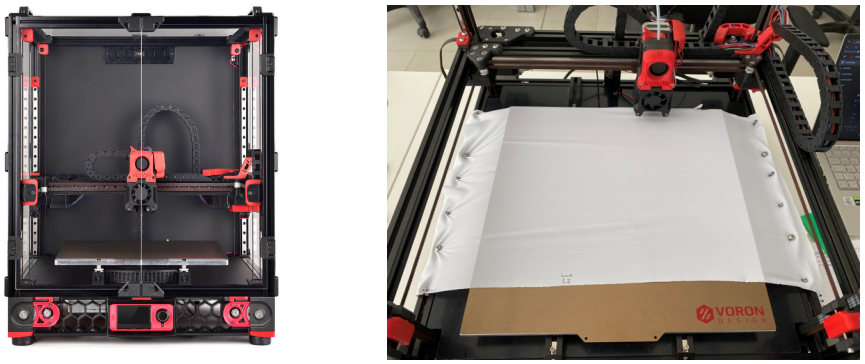

Figure 1. The VORON 2.4 3D printer used in this study, and a preliminary setup to stretch the Lycra sheet exploiting the printer frame.

PLA is derived from the fermentation of carbohydrates found in corn performed by bacteria. The production process can allow for the control of the mechanical properties of the final product through nanotechnology, for example, by incorporating different fibers or nanofillers. PLA is biodegradable, with the degradation mediated by microorganisms under certain environmental conditions. Its main downside is, however, represented by its brittleness, though this issue did not provide any constraints to the outcome of the current activity.

Lycra, also known as Spandex and Dorlastan, is the commercial name of elastane fibers. These fibers contain a polyurethane bond, and they are used when elasticity and deformation recovery are highly required. Yarns made of Lycra are often spun together with yarns of natural fibers, to obtain elastic knitted fabrics with elongation at failure increasing with the percentage of the elastane.

This study was based on former tests performed to optimize the whole manufacturing process, in terms of the following parameters:

- Layer height, to set the vertical thickness of each deposited layer of PLA. It affects the quality of the product and the printing time.
- Wall thickness, to set the in-plane width of the printed parts. It affects the strength of the product, the printing time, and the amount of material used.
- Printing speed, to define the speed at which the extruder moves while printing. A higher printing speed increases the vibrations and makes the printed parts susceptible to under- and over-extrusion.
- Traveling speed, to define how fast the nozzle moves over the substrate to reach the next printing coordinates. It can be set much higher than the print speed, as it does not affect the print quality much, while it helps prevent oozing.
- Z-Hop, enabled to allow the nozzle to be lifted during traveling and avoid contact between the nozzle and the printed part. It makes printing more reliable, although slightly more time-consuming.
- Printing temperature, to define the temperature reached by the nozzle. It has to be high enough to melt the PLA filament, but it can also affect the viscosity of the Lycra substrate causing permanent unwanted deformations.

- Retraction: when the 3D printer stops pushing the material, the flow does not immediately stop, causing unwanted oozing and stringing. To define the retraction parameters, such as distance and speed, it has to be considered that retraction completely stops material flow, thus effectively preventing oozing, but it may also negatively affect dimensional accuracy and gripping.
- Cooling, which plays a significant role in setting the print quality, especially for materials with low glass transition temperature ranges such as PLA. Turning on the cooling option activates the fans, whose rotations remove heat from the deposited layer, allowing it to solidify before the next layer is deposited.

2.2. Finite Element Analysis

To validate the 3D printing process and optimize the performance of the stiffeners, FE analyses were run with the state-of-the-art FE software Abaqus [16], which stands as a powerful tool for performing parametric studies.

To match the real behavior of the printed structures, the same steps of the laboratory tests were considered: pre-stretching of the Lycra sheets; 3D printing of PLA stiffeners on the pre-stretched substrate; release of the pre-stretch to obtain the buckled configuration. Out of these three steps that characterize the 3D printing scheme, it turned out that the most challenging one to model was indeed the release of the pre-stretch of the Lycra sheet. In fact, by releasing the boundary conditions on its sides, the sheet turned out to be weakly constrained; further than that, the interface between the soft substrate and the hard printed part could lead to some wrinkles in the sheet. Hence, to fully model the release of the said boundary conditions, some energy stabilization had to be added to the analyses to obtain the results shown in the following and many more for data augmentation purposes, independently of the printed pattern.

Dynamic or inertial effects were disregarded in the present investigation, having assumed the pre-stretch to be applied and removed smoothly and slowly. Independently of the thicknesses, both the substrate and the printed stiffeners were discretized using hexahedral, 3D solid elements; a preliminary mesh refinement investigation was also carried out to make sure that the proper response of the system in bending could be attained for all the considered geometries.

2.3. Deep Learning

The NN-based DL strategy adopted here was split into two distinct parts, as already outlined. Here, we delve deeper into the functionality of each part, to understand the relevant role in predicting the buckled configurations. A kind of multi-fidelity approach was assumed, to exploit both laboratory data and the results of the FE analyses, each with the proper level of fidelity, see e.g., [10].

The first component of the proposed DL strategy exploited a pre-trained YOLO architecture [17], adapted to recognize the three geometries characterizing the printed patterns: lines, rectangles, and crosses. This adaptation was obtained through an extensive re-training process on a custom-built dataset generated via matplotlib, allowing for diverse configurations of the target geometries. The YOLO model turned out to be able to identify each geometry within bounding boxes, which were then converted into the actual in-plane dimensions of the 3D printed part by way of a proper scaling factor. This scaling was imperative to maintain dimensional consistency across all the processed images and ensure the integrity of data input for the subsequent predictive modeling phase, as the said dimensions represent the crucial input parameters for the subsequent deformation-predictive NN.

For computational efficiency, the second part of the proposed DL strategy was divided into three sub-networks, each dedicated to one of the recognized geometries. This splitting of the information and, therefore, of the implementation was based on the premise that each printed geometry leads to a peculiar deformation response under similar boundary/loading conditions. Despite the aforementioned splitting, the structure of the sub-networks re-

mained consistent across the three geometries. Each network was designed to receive as input specific dimensional data: two parameters (width and thickness) for lines and three parameters (height, width and thickness) for rectangles and crosses.

The NNs were fully connected ones, with a single hidden layer featuring 32 neurons and with a single output that predicts the out-of-plane deflection in a specific point selected to characterize the printed pattern. The parameters of these NNs were initialized using the Glorot uniform initializer, which is particularly effective in maintaining a uniform scale of gradients across layers in DL models. A linear activation function was employed to account for the linear relationship observed between the input dimensions and the deformation in the FE simulations. As a loss function, for all the geometries, the mean squared error was employed to quantify the deviation of the digital predictions from the ground truth values.

3. Results and Discussion

The 3D printing setup was customized with a configuration of screws to link the Lycra sheet with the left and right sides of the bed, see Figure 1. An additional frame was also designed to allow changing the pre-stretch during the printing, so that multiple buckled configurations can be obtained at the same time. The fabric was locked into place and stretched in one single direction, although a biaxial stretching is possible and will be investigated in future activities, to understand the interplay between the fabric of the textile and the printed geometry of the stiffeners. A precise tuning of the value of the pre-stretch was allowed by an ad hoc designed system of movable (rotating) parts attached to the frame and constraining the membrane. As far as the printing parameters listed in Section 2.1 are concerned, their values as set in the experimental campaign are listed in Table 1. Some exemplary geometries of the printed parts and of the relevant buckled configurations can be seen in Figure 2.

In the FE analyses, PLA was assumed to behave elastically, featuring a Young's modulus $E = 3$ GPa and a Poisson's ratio $\nu = 0.25$. Due to its hyperelastic properties, see, e.g., [18], Lycra was instead assumed to behave according to the Arruda–Boyce model with the following values for the parameters, see [19]: $\mu = 9$ MPa, $\lambda_m = 87$ MPa, and $D = 0$. Results related to the exemplary geometries considered in Figure 2 are reported in Figure 3, as obtained by allowing for the symmetries in the geometry and boundary conditions so that only one quarter of the entire system was modeled.

Table 1. Values of printing parameters adopted in the present study.

Parameter	Value
Layer height (mm)	0.2
Layer width (mm)	0.4
Wall thickness (mm)	0.8
Top/Bottom pattern (-)	Concentric
First layer speed (mm/s)	20
Printing speed (mm/s)	30
Printing temperature (°C)	205
Bed temperature (°C)	30
Cooling fan (%)	100
Travel speed (mm/s)	150
Retraction (mm/s)	0.5
Z-Hop (mm)	0.3

Figure 2. Exemplary geometries of the 3D printed stiffeners.

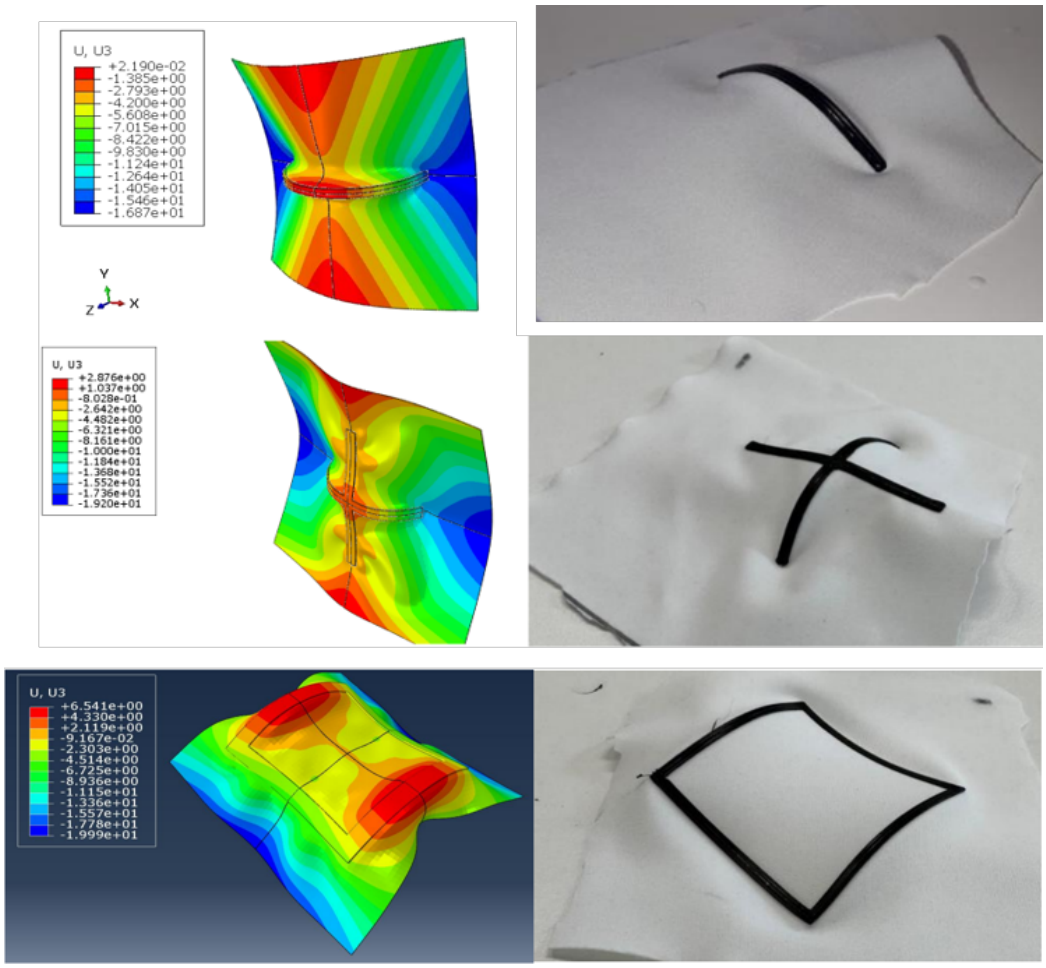

Figure 3. Comparison between the experimentally observed and the numerically obtained buckled configurations, related to the exemplary geometries of stiffeners shown in Figure 2.

The YOLO model correctly identified each geometry within the bounding boxes, see Figure 4. The subsequent regression NNs were trained using a curated dataset collecting the results of the FE simulations, encompassing approximately 100 samples with different dimensions. The YOLO-based geometric recognition phase achieved a precision of 93% and a recall of 99% at a 0.2 level of confidence, a threshold at which the identification of geometries can be considered reliable, see Figure 5. This high level of accuracy ensured that the dimensions fed into the deformation prediction NNs were based on dependable preliminary recognition, laying a solid foundation for subsequent predictive accuracy. For all the geometries, the error assessment was conducted on randomly selected samples representing 20% of the training dataset, to perform a validation test. The mean absolute percentage error (MAPE) evaluated on these samples yielded an outcome that testifies the procedure's performance under the proposed training conditions: in particular, a MAPE of 2.67%, 3.80%, and 5.13% was attained for the datasets composed of lines, crosses, and rectangles, respectively.

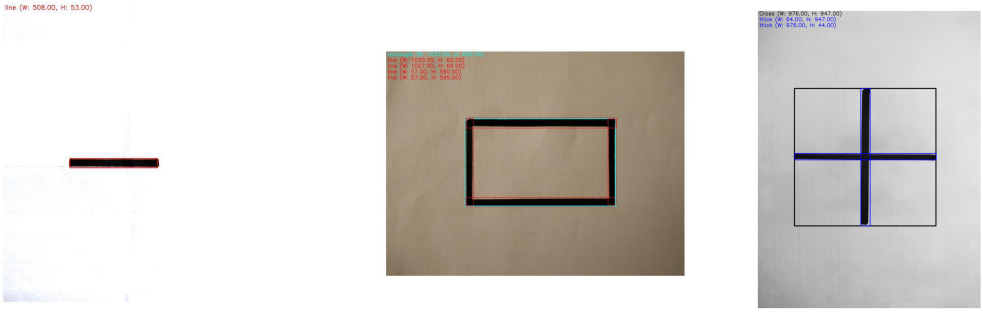

(**a**) (**b**) (**c**)

Figure 4. Exemplary YOLO outputs for the three different geometries. In the figures, different colors of the bounding boxes correspond to the different geometries identified, in the case of (**a**) line, (**b**) rectangle, and (**c**) cross geometries.

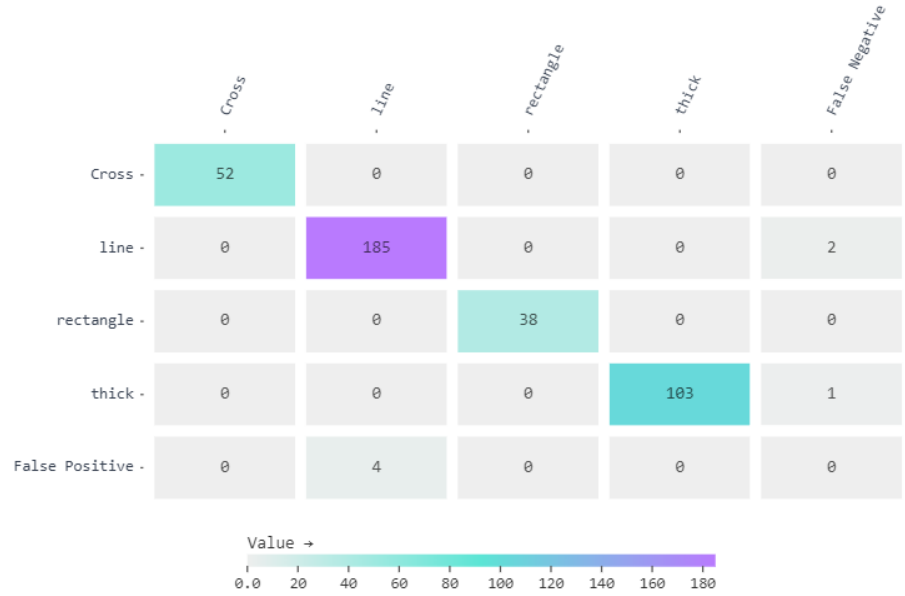

Figure 5. Confusion matrix evaluated at 0.2 confidence threshold on validation and test datasets, leading to a precision of 93% and a recall of 99%.

4. Conclusions

Despite the challenges envisioned for printing hard stiffeners on pre-stretched compliant membranes and for learning how the system buckles as soon as the mentioned pre-stretch is released, the results gathered here can be considered promising to provide proof of the capability of the proposed NN-based approach. This would become especially important when moving to more complex 3D printed patterns, as numerical simulations can become unfeasible and too expensive to be used as the only basis for the optimization strategy of the geometry.

Future efforts will focus on enhancing the dataset with a more balanced range of geometric dimensions. The learning scheme, which has been slightly discussed in the paper, will be further investigated to understand whether weights can be shared among the NNs used for the different geometries. To extend the proposed methodology to other geometric types, a reduction in the MAPE is foreseen to improve the robustness and reliability of model predictions.

Author Contributions: Conceptualization, S.M.; methodology, S.B., D.C., P.M. and S.M.; software, S.B., P.M. and A.T.; validation, S.B., P.M., A.T. and S.M.; formal analysis, S.B., P.M. and A.T.; investigation, S.B., P.M. and A.T.; resources, S.M.; writing—original draft preparation, P.M. and S.M.; writing—review and editing, A.T. and S.M.; visualization, P.M.; supervision, D.C. and S.M.; project administration, S.M. All authors have read and agreed to the published version of the manuscript.

Funding: This research received no external funding.

Institutional Review Board Statement: Not applicable.

Informed Consent Statement: Not applicable.

Data Availability Statement: The data presented in this study are available on request from the corresponding author.

Conflicts of Interest: The authors declare no conflict of interest.

References

1. Markus Henke, E.-F.; Wilson, K.E.; Anderson, I.A. Entirely soft dielectric elastomer robots. In *Electroactive Polymer Actuators and Devices (EAPAD)*; SPIE: Portland, OR, USA, 2017; Volume 101631.
2. Agkathidis, A.; Berdos, Y.; Brown, A. Active membranes: 3D printing of elastic fibre patterns on pre-stretched textiles. *Int. J. Archit. Comput.* **2019**, *17*, 74–87. [CrossRef]
3. Kycia, A.; Guiducci, L.; Werner, L.; Koering, D. Self-shaping Textiles—A material platform for digitally designed, material-informed surface elements. In Proceedings of the Anthropologic: Architecture and Fabrication in the Cognitive Age—Proceedings of the 38th eCAADe Conference, Berlin, Germany, 16–18 September 2020; Volume 2, pp. 21–30.
4. Korger, M.; Bergschneider, J.; Lutz, M.; Mahltig, B.; Finsterbusch, K.; Rabe, M. Possible Applications of 3D Printing Technology on Textile Substrates. In Proceedings of the IOP Conference Series: Materials Science and Engineering, Volume 141, 48th Conference of the International Federation of Knitting Technologists (IFKT), Moenchengladbach, Germany, 8–11 June 2016; p. 012011
5. Oxman, N.; Rosenberg, J.L. Material-based Design Computation An Inquiry into Digital Simulation of Physical Material Properties as Design Generators. *Int. J. Archit. Computing*. **2007**, *5*, 25–44. [CrossRef]
6. Bazant, Z.P.; Cedolin, L. *Stability of Structures: Elastic, Inelastic, Fracture and Damage Theories*; World Scientific Publishing: Singapore, 2010.
7. Koch, H.C.; Schmelzeisen, D.; Gries, T. 4D Textiles Made by Additive Manufacturing on Pre-Stressed Textiles—An Overview. *Actuators* **2021**, *10*, 31. [CrossRef]
8. Rastogi, P.; Kandasubramanian, B. Breakthrough in the printing tactics for stimuli-responsive materials: 4D printing. *Chem. Eng. J.* **2019**, *366*, 264–304. [CrossRef]
9. Arshad, V.; Jamil, B.; Rodrigue, H. FlexiStiff: A Variable Tensile Stiffness Element for Modulating the Behavior of Tensegrity Structures. *Adv. Eng. Mater.* **2024**, *26*, 2400497. [CrossRef]
10. Torzoni, M.; Manzoni, A.; Mariani, S. A multi-fidelity surrogate model for structural health monitoring exploiting model order reduction and artificial neural networks. *J. Mech. Syst. Signal Process.* **2023**, *197*, 110376. [CrossRef]
11. Uludag, M.; Ulkir, O. Optimizing surface roughness in soft pneumatic gripper fabricated via FDM: Experimental investigation using Taguchi method. *Multidiscip. Model. Mater. Struct.* **2024**, *20*, 211–225. [CrossRef]
12. Ulkir, O.; Bayraklılar, M.S.; Kuncan, M. Raster Angle Prediction of Additive Manufacturing Process Using Machine Learning Algorithm. *Appl. Sci.* **2024**, *14*, 2046. [CrossRef]
13. Quesada Molina, J.P.; Mariani, S. ybrid model-based and data-driven solution for uncertainty quantification at the microscale. *Micro Nanosyst.* **2022**, *14*, 281–286. [CrossRef]
14. Yuan, Z.; Zhu, S.; Mariani, S.; Zhang, Q.; Wu, J.; Zhai, W. Unsupervised cross-domain damage detection and localization for vibration isolators in metro floating-slab track. *Mech. Syst. Signal Process.* **2023**, *200*, 110647. [CrossRef]
15. Jourdan, D.; Skouras, M.; Vouga, E.; Bousseau, A. Printing-on-fabric meta-material for self-shaping architectural models. In Proceedings of the Advances in Architectural Geometry 2020, Paris, France, 28–29 April 2021.
16. *ABAQUS/Standard User's Manual*; Dassault Systèmes Simulia Corp: Providence, RI, USA, 2024.
17. Redmon, J. You Only Look Once: Unified, Real-Time Object Detection. In Proceedings of the 2016 IEEE Conference on Computer Vision and Pattern Recognition (CVPR), Las Vegas, NV, USA, 27–30 June 2016; pp. 779–788.
18. Belytschko, T.; Liu, W.K.; Moran, B.; Elkhodary, K. *Nonlinear Finite Elements for Continua and Structures*, 2nd ed.; Wiley-Blackwell: Oxford, UK, 2014.
19. Arruda, E.M.; Boyce, M.C. A three-dimensional model for the large stretch behavior of rubber elastic materials. *J. Mech. Phys. Solids* **1993**, *41*, 389–412. [CrossRef]